A&A 440, 783–789 (2005)
DOI: 10.1051/0004-6361:20042012

Astronomy & Astrophysics

A survey for OB associations in the Sculptor Group spiral galaxy NGC 7793⋆,⋆⋆

G. Pietrzyński[1,2], K. Ulaczyk[2], W. Gieren[1], F. Bresolin[3], and R. P. Kudritzki[3]

[1] Universidad de Concepción, Departamento de Fisica, Casilla 160–C, Concepción, Chile
e-mail: pietrzyn@hubble.cfm.udec.cl; wgieren@astro-udec.cl
[2] Warsaw University Observatory, AL. Ujazdowskie 4, 00-478 Warsaw, Poland
e-mail: kulaczyk@astrouw.edu.pl
[3] Institute for Astronomy, 2680 Woodlawn Drive, Honolulu, HI 96822, Hawaii, USA
e-mail: [bresolin; kud]@ifa.hawaii.edu

Received 15 September 2004 / Accepted 13 April 2005

Abstract. We report on the results from application of an objective algorithm (PLC) to find OB associations, to *B* and *V* images of the Sculptor spiral galaxy NGC 7793, which were obtained with the ESO VLT and FORS instrument and basically cover the entire spatial extent of the galaxy. We detected 148 associations. Statistical tests show that less than 6 of these detections are caused by randomly concentrated blue stars. In the size distribution, a sharp peak is observed at a value of about 35 microradians, which corresponds to a linear diameter of 135 pc, assuming a distance of 3.91 Mpc to the galaxy. We also find 25 much larger objects. A second application of the PLC technique shows that 20 of them are stellar complexes consisting of multiple subassociations with typical sizes on the order of 130 pc. A comparison of the size distribution of the detected OB associations in NGC 7793 with observed distributions in other galaxies suggests that the conditions in two Sculptor Group galaxies (NGC 300 and NGC 7793) favour the formation of large associations. We provide a catalog giving coordinates and physical parameters for all the associations and stellar complexes we have found in our survey.

Key words. Galaxy: open clusters and associations: individual: galaxy: NGC 7793

1. Introduction

OB associations consist of young massive stars formed from the same molecular cloud. Their members are very hot and gravitionally unbound. It is well known that OB associations are important because they can provide valuable hints about star formation processes in galaxies, and are the tracers of recent or current massive star formation in their host galaxies. Star formation is the primary process in shaping the evolution of a galaxy, not only by the addition of new stars. Young massive stars also strongly influence the surrounding interstellar environment through their stellar winds and supernova explosions. It still needs to be understood how large-scale mechanisms govern the production of stars and distribution of gas in a galaxy. Analyzing the properties of OB associations and observing how these properties are connected to the global galaxy characteristics is a basic observational input to understand how massive stars form and how they contribute to the chemical evolution of their host galaxies.

Identification of stellar associations in galaxies has been a difficult problem because, as pointed out by Hodge (1986), results based on visual judgement are very subjective, and strongly dependent on the observational material available. Hodge was able to experimentally show that two different authors recognize different stellar associations from the same observational material. In fact, the very low surface density of associations makes their identification by a density contrast with the background impossible. This problem, in addition to non-uniform and often low-quality observational data, has frequently caused disagreements among various authors.

The need for an objective technique to identify OB associations was obvious and several methods based on different parameters have been proposed up to now. The "friends of friends" technique (Wilson 1991) and the The Path Linkage Criterion, PLC algorithm (Battinelli 1991) turned out to be particulary useful. A brief discussion of the differences between Battinelli's (1991) and Wilson's (1992) techniques is given in Battinelli & Demers (1992) and also in Wilson (1992). The main advantage of using the PLC algorithm is that this procedure allows to derive automatically, from the observed stellar distribution, a unique value for the search radius (see Sect. 3), while in the Wilson's approach it remains a

⋆ Based on observations obtained with the VLT telescope at the ESO Paranal Observatory, Chile as part of project 69.D-0041.
⋆⋆ Table 1 is only available in electronic form at http://www.edpsciences.org

free parameter. Because of this, and since the PLC algorithm has been successfully tested in several nearby galaxies, providing reliable identifications of extragalactic OB associations (Battinelli 1991; Bresolin et al. 1998; Pietrzynski et al. 2001, and references therein) and we have used it in our previous work on another Sculptor Group galaxy, NGC 300 (Pietrzynski et al. 2001), we adopted it to conduct a survey OB associations in the spiral galaxy NGC 7793, which is the subject of this paper. NGC 7793, an Sd galaxy at a distance of 3.91 Mpc (Karachentsev et al. 2003), is about twice the distant of NGC 300 (Gieren et al. 2004), making the detection of its OB associations slightly more difficult.

2. Observations, photometry and equatorial coordinates

The observations were performed during two photometric nights in July 2001 with the ESO VLT and FORS1 instrument (see ESO website for details) in imaging mode. The FORS1 field of view is approximately 6.8×6.8 arcmin, and the pixel scale of the FORS1 detector is 0.2 arcsec/pix. We obtained images in B, V, I, and H_α filters for two fields, which together cover almost the entire galaxy (see Fig. 1). The data were obtained under 1 arcsec seeing conditions.

The raw frames were debiased and flat-fielded in the standard way using the IRAF[1] package. The PSF photometry and aperture corrections were obtained with the DAOPHOT/ALLSTAR programs in the same manner as described by Pietrzyński et al. (2002). The accuracy of the aperture corrections was better than 0.02 mag.

In order to transform our instrumental magnitudes to the standard *BVI* system, several Landolt fields were also imaged on both nights together with our targets. Based on these data the following transformations were established:
Night 1:

$$B = b - 0.071 \times (B - V) + \text{const.}_B$$
$$V = v + 0.036 \times (V - I) + \text{const.}_V$$

Night 2:

$$B = b - 0.084 \times (B - V) + \text{const.}_B$$
$$V = v + 0.033 \times (V - I) + \text{const.}_V.$$

The lower case letters b and v in these equations denote the aperture magnitudes normalized to 1 s exposure time. The derived color coefficients are small, which indicates that our instrumental system closely matches the standard one. They are also very close-to-the-mean color coefficients obtained at Paranal during 2001 (e.g. −0.084 for B and 0.029 for V, see `www.eso.org`). The residuals were not larger than 0.05 mag and did not show any significant dependence on color, brightness, or position on the sky. The accuracy of the zero points was estimated to be about 0.04 and 0.05 mag for the two bands for the first and second nights, respectively.

[1] IRAF is distributed by the National Optical Astronomy Observatories, which are operated by the Association of Universities for Research in Astronomy, Inc., under cooperative agreement with the NSF.

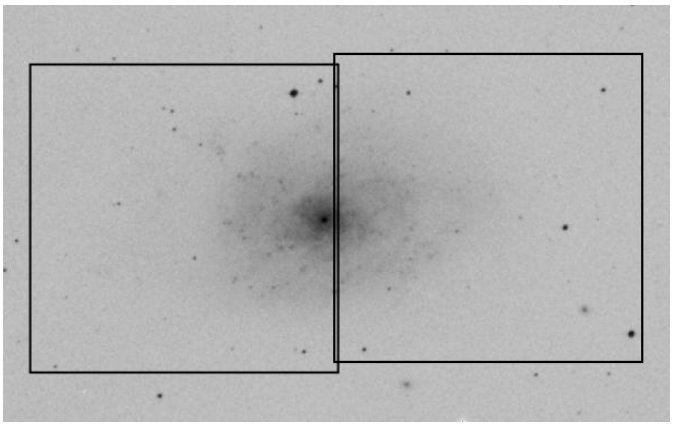

Fig. 1. V images of the two fields in NGC 7793 observed with VLT/FORS. The images cover most of the visible spatial extent of the galaxy.

The coordinates of all stars were converted to the equatorial system based on images from DSS-2 Survey in an identical manner to Udalski et al. (1998).

3. Search for associations

3.1. Identification method

In our analysis we used the original PLC code (Battinelli 1991), kindly privided us by Dr. Battinelli. The main assumption of this technique is that two stars belong to the same association, if it is possible to link them by subsequently connecting stars between them, whose distance from each other is not larger than a certain parameter, called search radius d_s. An optimum value of d_s can be calculated using a function $f_p(d)$, which gives the number of associations containing at least p stars detected using the distance parameter d. Increasing d from zero causes a growth of f, which means that at a given distance stars begin to group, until $f_p(d)$ reaches a maximum value. Then $f_p(d)$ starts to decrease towards a limiting value of 1, which corresponds to the connection of all stars into one big association. The optimum value of the search radius is that at which the function $f_p(d)$ reaches its maximum.

3.2. Aplication of the automatic technique

Before we apply the PLC technique we must select blue stars from our galaxy, which simply means that we need to define a range of brightness and color on the CMD diagram. The following criteria were used: $V < 23.3$ mag and $-0.6 < B - V < 0.4$ mag. Our requirements were fulfilled by 3908 stars out of the 6709 stars for which photometric V, $B - V$ data were obtained in this study. We present our selection in Fig. 2.

It is worth noting that the location of NGC 7793 on the sky implies a very low foreground reddening, so the unreddened color cutoff is almost unchanged (Burstein & Heiles 1984). Assuming for the distance modulus for NGC 7793 the value obtained by Karachentsev et al. (2003) (3.91 Mpc, corresponding to 27.96 mag), our brightness cutoff in absolute scale equals $M_V = -4.7$ mag, in the sense that we retain for analysis all

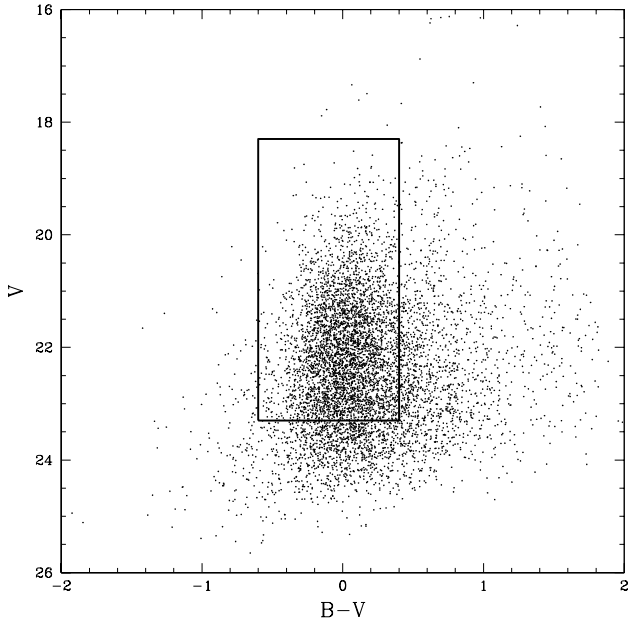

Fig. 2. Color-magnitude diagram for NGC 7793, constructed from 6709 stars with B, V photometry from our VLT FORS images. The inserted rectangular box contains the blue stars used for our search of OB associations.

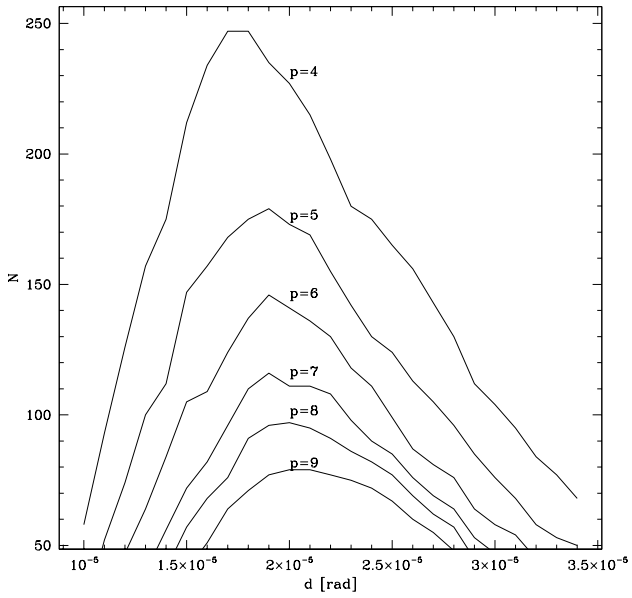

Fig. 3. The $f_p(d)$ function, obtained for different values of the p parameter (see explanation in text).

detected stars in the chosen color range more luminous than this value.

Before using the PLC technique to detect OB associations, one needs to adopt values for several important parameters. As mentioned above, the first parameter that needs to be determined is d_s. In order to do that, we applied the PLC technique to our data using several values of the distance parameter, and of the minimum number of stars that compose an association. Figure 3 presents the results of this excercise. One can clearly see that the maximum of the function $f_p(d)$ is located close to about 1.9×10^{-5} and depends very little on the

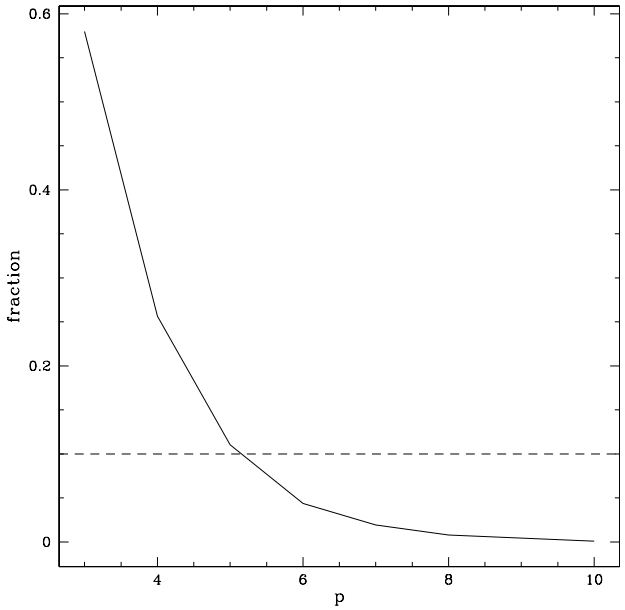

Fig. 4. The fraction of spurious detections as function of the minimum number of stars belonging to an association.

chosen value of p. To find a more precise value of d_s, we increased the resolution of our calculations around the value of 1.9×10^{-5} rad (for $p = 5, 6, 7$) and obtained a final best value of $d_s = 1.89 \times 10^{-5}$ rad.

The next problem is related to finding the most appropriate value of the parameter p. If we choose too small a number of stars, we will get many detections caused by coincidence. On the other hand, if we demand too large a number of stars, many compact associations will be missed. To find the best solution to this problem, the following statistical test was performed. A random distribution of the number of stars equal to the number of selected blue stars over the observed area was generated and then searched for groups adopting $d_s = 1.89 \times 10^{-5}$ rad, and several different values for p. In order to get reasonable statistics, we repeated this one hundred times. The resulting fraction of spurious detections (the mean number of groups found in random distributions) to the total number of associations detected with the same parameters is shown in Fig. 4. We demand that spurious detections constitute less then 10 percent of the total number of detections, so 6 seems to be an adequate value for the minimum number of stars in an OB association.

Our adopted selection criteria are identical to those used by Pietrzyński et al. (2001) and very similar to the criteria used in other surveys for OB associations (e.g. Bresolin et al. 1998).

4. Results

4.1. The catalog

Finally, we applied the PLC technique to our catalog of blue stars with our chosen parameters p and d_s. It resulted in the detection of 148 associations catalogued in Table 1. In subsequent columns, the catalog contains: identification, right ascension, declination, number of stars in the association, angular size in microradians, and linear size in parsecs. The coordinates of the

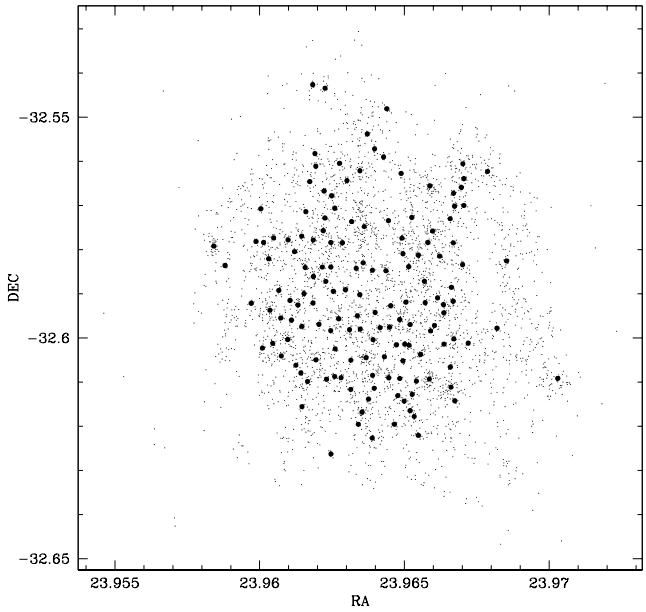

Fig. 5. Distribution of the detected OB associations (black circles) over the disc of NGC 7793, which is traced out by the blue stars (dots).

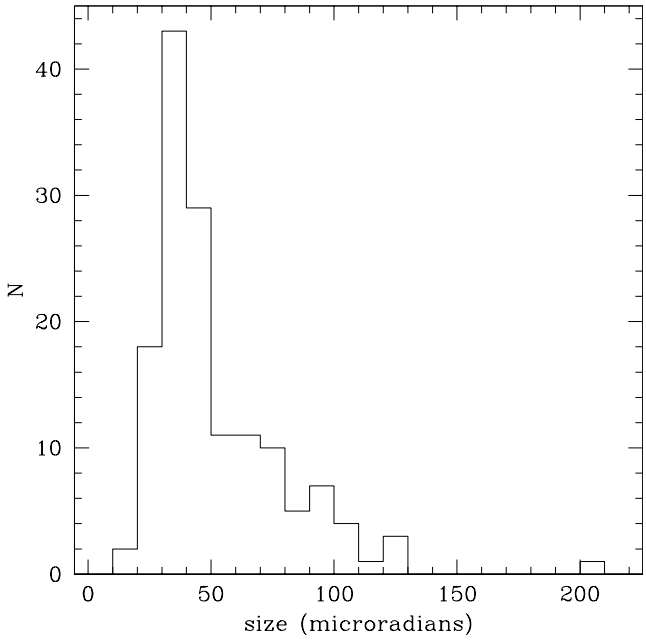

Fig. 6. Observed distribution of the angular sizes of detected OB associations in NGC 7793.

given associations are the mean coordinates of their member stars. According to Battinelli (1991), the true diameter of an association is defined as $0.5*(\Phi_{\rm RA}*\cos(\Phi_{\rm Dec})+\Phi_{\rm Dec})*d_{\rm NGC\ 7793}$, where $\Phi_{\rm RA}$ and $\Phi_{\rm Dec}$ are diameters in both coordinates, and $d_{\rm NGC\ 7793}$ corresponds to the distance to NGC 7793, assumed to be 3.91 Mpc. The spatial distribution of our detected associations over the disc of the galaxy is shown in Fig. 5.

A powerful check for the reality of the detected OB associations is their correlation with regions of ionized hydrogen, which are formed by the UV photons emitted from the young and massive stars. Unfortunately, to our knowledge no published catalog of H II regions exists for NGC 7793, so to cross-correlate the positions of the detected OB associations with those of H II regions in NGC 7793, we used our own H_α images, which were also obtained with VLT/FORS. After marking our detected OB associations on the H_α images, we found by careful visual inspection that the positions of 104 OB associations, out of the 148 detected ones, do in fact coincide with H II region candidates. This high coincidence rate of about 70% supports the physical reality of our detected OB associations; a higher rate of coincidence can probably not be expected since it is known that not all associations are connected to visible H II regions.

In Fig. 6, we show the size distribution of the OB associations detected and measured from our data. It resembles a sharp peak at about 35 microradians, which corresponds to a true diameter of 137 pc with the adopted NGC 7793 distance of 3.91 Mpc.

4.2. Superassociations

Looking at the histogram of sizes (Fig. 6), we can clearly see that the associations are separated into two categories. The first consists of typical OB associations with sizes around 100−150 pc, whereas the second contains associations with sizes larger than 300 pc. It was visually checked that most of these large stellar groups are actually stellar complexes, which consist of several smaller associations. These were not detected as individual groupings of stars by our algorithm because of the high density of blue stars in these regions. To provide an objective proof, we applied the PLC algorithm to these complexes. It turned out that in 20 out of 25 cases these complexes indeed consist of a number of smaller associations with typical sizes around 100 pc. Results are shown in Table 2. The designations of these subassociations were created from the identification of their host associations by the addition of roman letters. The remaining columns are organized in the same way as in Table 1. These stellar complexes, like the detected associations, are distributed rather uniformly over the galaxy disc.

5. Discussion

In order to obtain clues for understanding the processes which govern the formation of OB associations and, in particular, of early type stars, it is useful to compare the size distributions of objectively selected OB associations in galaxies which have very different environments. Such a comparison was already performed by Bresolin et al. (1998) for some Local Group galaxies and seven more distant spirals (NGC 925, NGC 3621, NGC 2541, NGC 4548, NGC 3351, NGC 2090, and M 101) observed with the Hubble Space Telescope in the course of the Key Project on the distance scale. The main result of this comparison was that the properties of OB associations (size distribution; their average diameter, found to be about 80 pc) do not vary significantly between Local Group galaxies and all studied spirals.

In order to do a similar comparison for Sculptor Group galaxies we searched the literature for a sample of catalogs of OB associations in nearby, well-resolved galaxies in the

Table 2. Catalog of detected OB associations in NGC 7793 belonging to stellar complexes.

Name	α_{2000}	δ_{2000}	N	Size [μrad]	Size [pc]
AS_4a	$23^h57^m59.3^s$	–32°36′43″	15	55	215
AS_4b	$23^h58^m0.1^s$	–32°36′37″	9	45	176
AS_7a	$23^h57^m48.6^s$	–32°34′33″	10	42	164
AS_7b	$23^h57^m48.5^s$	–32°34′16″	10	32	124
AS_7c	$23^h57^m50.5^s$	–32°34′38″	9	38	148
AS_7d	$23^h57^m49.3^s$	–32°34′26″	11	43	168
AS_7e	$23^h57^m49.0^s$	–32°34′41″	6	21	83
AS_7f	$23^h57^m48.6^s$	–32°34′10″	7	21	81
AS_7g	$23^h57^m48.5^s$	–32°34′46″	7	24	92
AS_9a	$23^h57^m59.5^s$	–32°35′34″	6	27	106
AS_9b	$23^h57^m59.2^s$	–32°35′41″	9	39	151
AS_13a	$23^h57^m57.7^s$	–32°34′37″	6	24	93
AS_13b	$23^h57^m56.8^s$	–32°34′33″	8	28	109
AS_15a	$23^h57^m56.9^s$	–32°33′54″	12	54	210
AS_15b	$23^h57^m57.6^s$	–32°33′59″	14	47	185
AS_16a	$23^h57^m48.7^s$	–32°36′17″	17	43	167
AS_16b	$23^h57^m49.3^s$	–32°36′14″	6	23	91
AS_17a	$23^h57^m49.0^s$	–32°36′34″	6	19	73
AS_17b	$23^h57^m50.8^s$	–32°36′26″	13	42	166
AS_17c	$23^h57^m49.8^s$	–32°36′33″	8	39	151
AS_19a	$23^h57^m56.8^s$	–32°35′19″	12	49	192
AS_19b	$23^h57^m56.3^s$	–32°35′12″	12	58	225
AS_20a	$23^h57^m54.3^s$	–32°35′25″	8	36	140
AS_20b	$23^h57^m54.1^s$	–32°35′38″	8	35	138
AS_23a	$23^h57^m54.1^s$	–32°34′39″	6	29	114
AS_23b	$23^h57^m53.6^s$	–32°34′40″	8	33	129
AS_26a	$23^h57^m55.6^s$	–32°36′15″	8	40	155
AS_26b	$23^h57^m56.4^s$	–32°36′10″	10	33	131
AS_45a	$23^h57^m55.9^s$	–32°34′46″	9	37	143
AS_45b	$23^h57^m55.8^s$	–32°34′55″	6	20	77
AS_48a	$23^h57^m56.7^s$	–32°36′35″	13	39	152
AS_48b	$23^h57^m57.1^s$	–32°36′30″	7	27	104
AS_50a	$23^h57^m59.9^s$	–32°35′58″	6	23	90
AS_50b	$23^h58^m0.1^s$	–32°36′6″	10	43	169
AS_50c	$23^h58^m0.6^s$	–32°35′54″	6	40	155
AS_85a	$23^h57^m45.7^s$	–32°35′51″	9	36	141
AS_85b	$23^h57^m46.0^s$	–32°35′36″	7	25	97
AS_85c	$23^h57^m45.5^s$	–32°35′42″	6	29	111
AS_87a	$23^h57^m39.2^s$	–32°35′59″	14	47	184
AS_87b	$23^h57^m40.1^s$	–32°36′7″	6	33	131
AS_95a	$23^h57^m36.8^s$	–32°35′32″	7	29	112
AS_95b	$23^h57^m37.3^s$	–32°35′43″	11	46	180
AS_100a	$23^h57^m42.3^s$	–32°36′34″	16	76	296
AS_100b	$23^h57^m41.3^s$	–32°36′40″	7	30	118
AS_102a	$23^h57^m41.6^s$	–32°34′59″	14	56	219
AS_102b	$23^h57^m41.9^s$	–32°35′9″	7	38	147
AS_105a	$23^h57^m42.3^s$	–32°36′17″	6	31	123
AS_105b	$23^h57^m43.2^s$	–32°36′16″	13	63	245
AS_105c	$23^h57^m43.5^s$	–32°36′29″	8	36	139

Local Group, which have been prepared with similar objective techniques based on ground-based data. The following catalogues were used for comparison: IC 1613 (Borissova et al. 2004), LMC (Bresolin et al. 1996), M 33 (Wilson 1991), NGC 6822 (Wilson 1992), SMC (Battinelli 1991), and M 31 (Magnier et al. 1993). The size distributions of OB associations

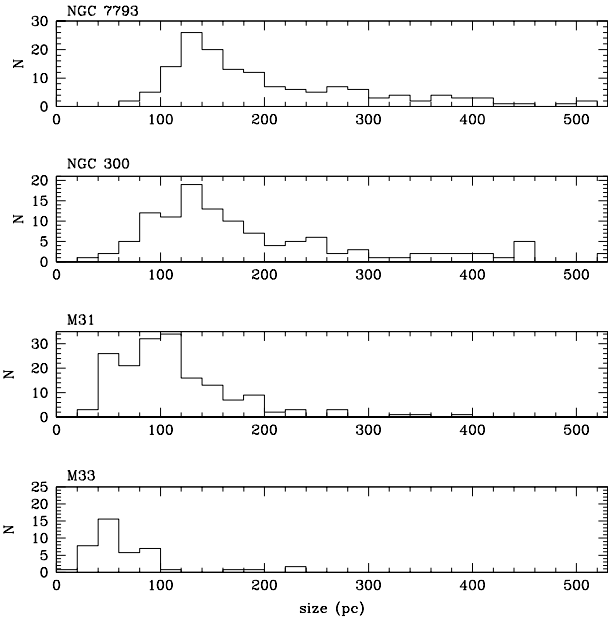

Fig. 7. Observed distribution of the linear sizes of OB associations for NGC 7793, NGC 300, M 31, and M 33.

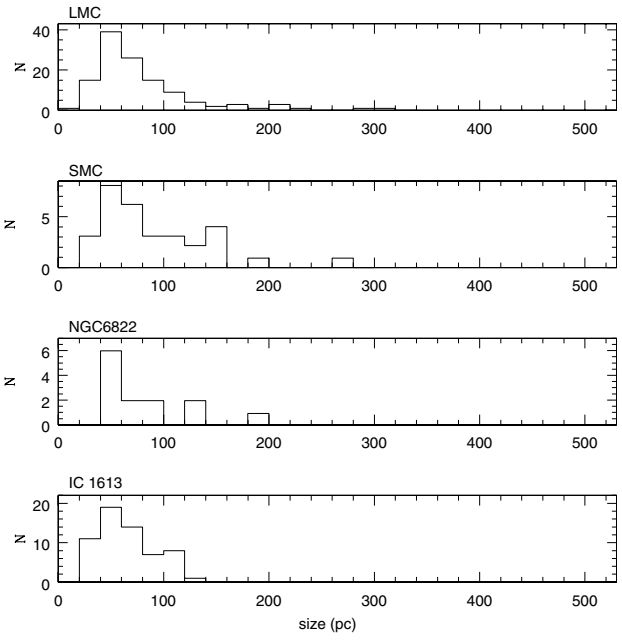

Fig. 8. Observed distribution of the linear sizes of OB associations for the LMC, SMC, NGC 6822, and IC 1613.

observed in these galaxies are presented in Figs. 7 and 8. Following suggestions made by the referee we also included, in our comparison the catalogs of OB associations in more distant galaxies aviable in the literature; namely, the results of study of association systems in seven spiral galaxies performed by Bresolin et al. (1998), the catalogs of associations in UGC 12732, NGC 1058, and NGC 7217 (Battinelli et al. 2000), and in NGC 4394, NGC 3507, and NGC 3377A (Vicari et al. 2002). Corresponding size distributions are displayed in Figs. 9 and 10, respectively.

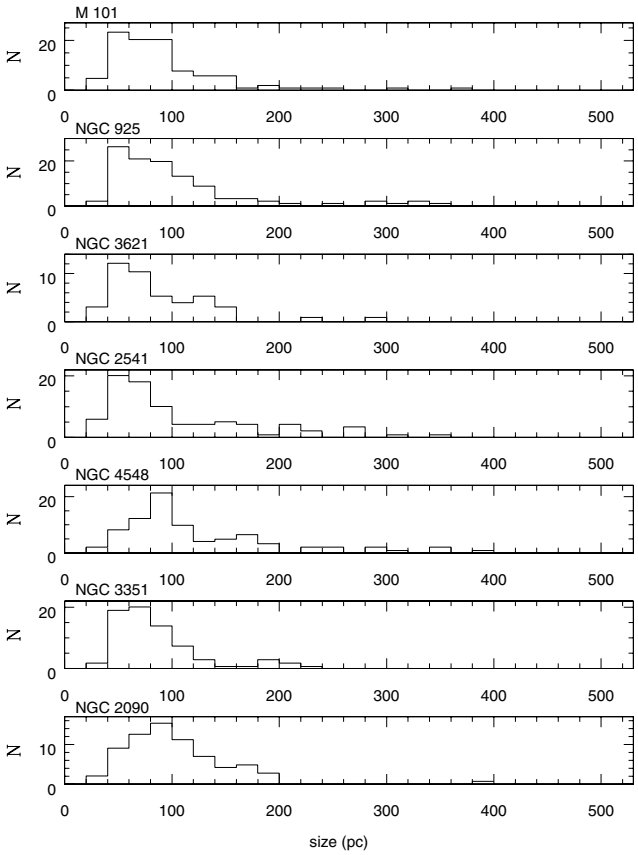

Fig. 9. Observed distribution of the linear sizes of OB associations for M 101, NGC 925, NGC 3621, NGC 2541, NGC 4548, NGC 3351, and NGC 2090.

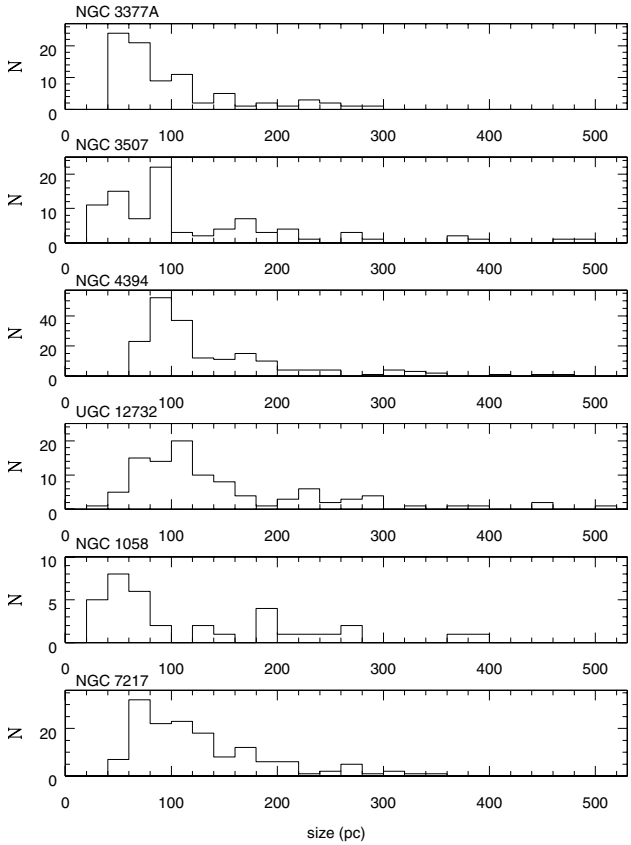

Fig. 10. Observed distribution of the linear sizes of OB associations for NGC 3377A, NGC 3507, NGC 4394, UGC 12732, NGC 1058, and NGC 7217.

Table 3. Basic information on number, sizes, and size distributions of OB associations in galaxies, as found in the literature.

Galaxy	Number of associations	Average diameter (pc)	Peak location (pc)	Associations with $D > 200$ pc
NGC 7793	148	207	130	55
NGC 300	117	195	130	37
M 31	174	118	110	13
M 33	41	40	50	2
IC 1613	60	63	50	0
LMC	121	78	50	6
SMC	31	90	50	1
NGC 6822	13	90	50	0
M 101	97	99	50	5
NGC 925	110	115	50	9
NGC 2090	70	104	90	1
NGC 2541	84	108	50	12
NGC 3351	73	87	70	3
NGC 3621	44	89	50	2
NGC 4548	82	125	90	10
NGC 1058	69	104	50	7
NGC 7217	149	129	70	21
UGC 12732	108	178	110	30
NGC 3377A	83	87	50	8
NGC 3507	90	121	90	16
NGC 4394	185	114	90	25

It should be noted here that following former studies (Bresolin et al. 1998; Pietrzynski et al. 2001), we present distributions of sizes of the associations detected in the first step of the PLC algorithm; e.g. we did not distinguish between associations and stellar complexes. However one should bear in mind that many groups of blue stars with larger sizes than about 200 pc consist of smaller objects with sizes typical of OB associations.

The basic information (total number of OB associations, their average diameter, location of the highest peak in the corresponding size distribution, and number of associations with diameter larger than 200 pc) about the system of associations in all selected galaxies is given in Table 3.

It is clearly seen that the distributions for the two Sculptor spirals NGC 300 and NGC 7993 are very similar to each other and different to other distributions presented in Fig. 8, in the sense that in NGC 300 and NGC 7793 significant fractions of the detected associations are large-sized, with diameters in excess of 200 pc, something not seen in the Irregular Local Group galaxies (NGC 6822, IC 1613, LMC, and SMC). Unfortunatelly, the catalogs of OB associations in M 33 and M 31 were based on observations that covered only limited subfields of these galaxies (3% and 25%, respectively), so they might not be representative of the entire galaxies, especially when considering large associations and complexes.

It is also evident that such large associations are less frequent in all distant spiral galaxies, selected from the literature

(see Figs. 9 and 10, and Table 3) than in our two Sculptor Group galaxies.

The average diameters of OB associations from NGC 7793 and NGC 300 (about 200 pc) are significantly larger than average diameters of OB associations in the Local Group (about 80 pc) and in more distant galaxies presented in the Table 3 (typically about 100 pc). The single exception is UGC 12732, where the average association diameter, 178 pc, is comparable to the corresponding values found for NGC 300 and NGC 7793.

The very small number of relatively small (smaller than 80 pc) associations in NGC 300 can be at least partly explained by the limited resolution of the images used for their detection. At the distance of NGC 300 ($m - M = 26.43$ mag, Gieren at al. 2004), associations with a linear size of 50 pc will have angular sizes of about 5 arcsec. The ground-based observations of this galaxy (Pietrzynski et al. 2001) were performed under seeing conditions of about 1 arcsec and many stars that are members of small associations could have been unresolved. As a consequence of such a situation, many small associations could have been missed due to fixing the parameter p. The situation is even worse in the case of the more distant NGC 7793 galaxy. In order to investigate the influence of blending on our results in more detail the following test was performed. We spatially degraded our images of NGC 300 as it would be located at the distance of NGC 7793 and searched for OB associations one more time. As a result about 5% of the small OB associations that had been detected on the original images were lost, which indicates that some fraction of the small associations may indeed be lost in our catalog of OB associations in NGC 7793 due to the limited spatial resolution of our images. Our results are very similar to those obtained by Bresolin et al. (1996), who found that spatial degradation by a factor of two of the HST images of M 101 caused the average size of detected associations to increase by about 10%.

An obvious way to investigate the true fraction of small-sized associations and therefore the correct average association diameter in the Sculptor galaxies would be to use HST images.

Acknowledgements. We would like to thank both Dr. Paolo Battinelli for providing us with his computer programs and the anonymous referee for many interesting suggestions which helped to improve this paper. G.P. and W.G. gratefully acknowledge financial support for this work from the Chilean Center for Astrophysics FONDAP 15010003. W.G. also acknowledges support from the Centrum fuer Internationale Migration und Entwicklung in Frankfurt/Germany, who donated the Sun Ultra 60 workstation on which a substantial part of the data reduction and analysis for this project was carried out. Support from the Polish KBN grant No. 2P03D02123 is also acknowledged.

References

Battinelli, P. 1991, A&A, 244, 69
Battinelli, P., & Demers, S. 1992, AJ, 104, 1458
Battinelli, P., Capuzzo-Dolcetta, R., Hodge, P. W., Vicari, A., & Wyder, T. K. 2000, 357, 437
Borissova, J., Kurtev, R., Georgiev, L., & Rosado, M. 2004, A&A, 413, 889
Bresolin, F., Kennicutt, R. C., & Stetson, P. B. 1996, AJ, 112, 2009
Bresolin, F., Kennicutt, R. C., Ferrarese, L., et al. 1998, AJ, 116, 119
Burstein, D., & Heiles, C. 1984, ApJS, 54, 33
Gieren, W., Pietrzynski, G., Walker, A., et al. 2004, AJ, 128, 1167
Hodge, P. W. 1986, in Luminous Stars and Associations in Galaxies, ed. C. W. H. De Loore, A. J. Willis, & P. G. Laskarides (Dordrecht: Reidel), IAU Symp., 116, 369
Karachentsev, I. D., Grebel, E. K., Sharina, M. E., et al. 2003, A&A, 404, 93
Larsen, S. S., & Richtler, T. 1999, A&A, 345, 59
Magnier, E. A., Battinelli, P., Lewin, W. H. G., et al. 1993, A&A, 278, 36
Pietrzynski, G., Gieren, W., Fouque, P., Pont, F., 2001, A&A 371, 497
Pietrzynski, G., Gieren, W., & Udalski, A. 2002, PASP, 114, 298
Udalski, A., Szymański, M., Kubiak, M., et al. 1998, Acta Astron., 48, 147
Vicari, A., Battinelli, P., Capuzzo-Dolceta, R., Wyder, T. K., & Arrabito, G., A&A, 384, 24
Wilson, C. D. 1991, AJ, 101, 1663
Wilson, C. D. 1992, ApJ, 386, L29

Online Material

Table 1. Catalog of detected OB associations in NGC 7793.

Name	α_{2000}	δ_{2000}	N	Size [μrad]	Size [pc]
AS_1	$23^h57^m48.9^s$	–32°34′59″	12	50	196
AS_2	$23^h57^m48.7^s$	–32°37′0″	19	63	245
AS_3	$23^h57^m54.7^s$	–32°36′59″	7	37	146
AS_4	$23^h57^m59.8^s$	–32°36′40″	36	129	505
AS_5	$23^h57^m54.0^s$	–32°36′51″	14	69	271
AS_6	$23^h57^m53.8^s$	–32°34′51″	11	64	252
AS_7	$23^h57^m49.0^s$	–32°34′29″	100	205	801
AS_8	$23^h58^m0.1^s$	–32°34′2″	7	34	135
AS_9	$23^h57^m58.9^s$	–32°35′39″	24	98	385
AS_10	$23^h57^m51.7^s$	–32°35′5″	21	71	277
AS_11	$23^h58^m0.1^s$	–32°35′30″	9	38	149
AS_12	$23^h57^m53.4^s$	–32°35′45″	17	70	273
AS_13	$23^h57^m57.5^s$	–32°34′33″	29	104	408
AS_14	$23^h57^m54.1^s$	–32°36′5″	6	19	72
AS_15	$23^h57^m57.2^s$	–32°33′56″	33	123	480
AS_16	$23^h57^m49.2^s$	–32°36′16″	38	96	374
AS_17	$23^h57^m50.0^s$	–32°36′30″	28	114	447
AS_18	$23^h58^m0.2^s$	–32°34′12″	11	41	159
AS_19	$23^h57^m56.5^s$	–32°35′14″	30	98	384
AS_20	$23^h57^m54.2^s$	–32°35′31″	27	99	386
AS_21	$23^h58^m1.1^s$	–32°33′57″	8	39	151
AS_22	$23^h58^m1.4^s$	–32°33′50″	8	27	107
AS_23	$23^h57^m53.7^s$	–32°34′39″	25	104	405
AS_24	$23^h58^m1.3^s$	–32°33′38″	7	44	170
AS_25	$23^h57^m50.3^s$	–32°33′26″	8	36	141
AS_26	$23^h57^m56.0^s$	–32°36′13″	21	84	327
AS_27	$23^h57^m50.1^s$	–32°36′1″	20	74	288
AS_28	$23^h58^m6.7^s$	–32°34′57″	8	43	167
AS_29	$23^h57^m52.1^s$	–32°36′33″	22	74	287
AS_30	$23^h57^m48.5^s$	–32°35′53″	11	41	160
AS_31	$23^h57^m50.4^s$	–32°35′39″	7	35	138
AS_32	$23^h57^m51.0^s$	–32°35′52″	12	48	186
AS_33	$23^h57^m55.2^s$	–32°37′4″	9	35	139
AS_34	$23^h57^m59.7^s$	–32°36′24″	6	34	131
AS_35	$23^h57^m53.2^s$	–32°36′47″	7	48	188
AS_36	$23^h57^m52.3^s$	–32°35′34″	9	44	174
AS_37	$23^h57^m50.0^s$	–32°35′5″	6	37	144
AS_38	$23^h58^m5.5^s$	–32°35′52″	6	34	134
AS_39	$23^h57^m54.9^s$	–32°34′22″	18	78	304
AS_40	$23^h57^m52.2^s$	–32°35′51″	8	33	128
AS_41	$23^h57^m48.2^s$	–32°35′42″	8	41	158
AS_42	$23^h57^m53.4^s$	–32°36′33″	6	34	133
AS_43	$23^h57^m54.7^s$	–32°35′49″	18	69	271
AS_44	$23^h57^m54.6^s$	–32°35′2″	6	34	133
AS_45	$23^h57^m55.7^s$	–32°34′52″	27	94	367
AS_46	$23^h57^m52.8^s$	–32°37′10″	8	41	161
AS_47	$23^h58^m0.1^s$	–32°34′42″	10	50	196
AS_48	$23^h57^m57.1^s$	–32°36′34″	41	108	422
AS_49	$23^h57^m55.7^s$	–32°37′19″	11	61	240
AS_50	$23^h58^m0.2^s$	–32°36′1″	22	85	333

Table 1. continued.

Name	α_{2000}	δ_{2000}	N	Size [μrad]	Size [pc]
AS_51	$23^h57^m48.5^s$	–32°35′25″	9	35	137
AS_52	$23^h57^m53.0^s$	–32°36′5″	6	29	114
AS_53	$23^h57^m58.1^s$	–32°35′27″	8	48	188
AS_54	$23^h57^m54.6^s$	–32°36′6″	9	33	129
AS_55	$23^h57^m58.9^s$	–32°36′5″	9	27	108
AS_56	$23^h58^m4.3^s$	–32°33′44″	14	81	317
AS_57	$23^h57^m58.9^s$	–32°35′33″	8	32	124
AS_58	$23^h58^m1.4^s$	–32°34′12″	7	38	150
AS_59	$23^h57^m58.4^s$	–32°34′53″	16	74	290
AS_60	$23^h58^m13.1^s$	–32°36′33″	6	25	96
AS_61	$23^h57^m48.5^s$	–32°33′44″	17	67	264
AS_62	$23^h57^m50.0^s$	–32°37′22″	6	28	111
AS_63	$23^h57^m56.9^s$	–32°34′42″	7	40	158
AS_64	$23^h57^m57.3^s$	–32°35′54″	6	33	129
AS_65	$23^h57^m55.0^s$	–32°36′46″	9	37	144
AS_66	$23^h57^m52.0^s$	–32°34′24″	6	31	121
AS_67	$23^h57^m55.5^s$	–32°36′35″	8	43	166
AS_68	$23^h57^m59.7^s$	–32°34′23″	8	39	151
AS_69	$23^h57^m53.8^s$	–32°36′19″	7	31	120
AS_70	$23^h57^m51.4^s$	–32°33′32″	6	20	79
AS_71	$23^h57^m51.8^s$	–32°32′53″	7	54	212
AS_72	$23^h57^m59.8^s$	–32°35′19″	8	40	158
AS_73	$23^h57^m51.5^s$	–32°36′15″	6	31	123
AS_74	$23^h58^m0.3^s$	–32°36′51″	6	42	163
AS_75	$23^h57^m56.6^s$	–32°35′31″	7	35	138
AS_76	$23^h57^m50.3^s$	–32°36′41″	8	37	143
AS_77	$23^h57^m49.5^s$	–32°36′50″	9	51	200
AS_78	$23^h58^m1.9^s$	–32°36′4″	7	47	183
AS_79	$23^h57^m57.7^s$	–32°35′50″	6	27	106
AS_80	$23^h57^m53.6^s$	–32°33′46″	10	56	220
AS_81	$23^h57^m48.0^s$	–32°35′3″	11	49	190
AS_82	$23^h58^m1.3^s$	–32°35′0″	8	26	100
AS_83	$23^h57^m49.4^s$	–32°33′14″	6	26	102
AS_84	$23^h57^m46.7^s$	–32°35′21″	12	48	190
AS_85	$23^h57^m45.8^s$	–32°35′44″	27	86	337
AS_86	$23^h57^m38.7^s$	–32°36′15″	16	58	225
AS_87	$23^h57^m39.5^s$	–32°36′1″	28	90	354
AS_88	$23^h57^m41.3^s$	–32°35′51″	10	44	173
AS_89	$23^h57^m41.2^s$	–32°34′37″	8	38	150
AS_90	$23^h57^m44.3^s$	–32°36′34″	12	59	230
AS_91	$23^h57^m46.3^s$	–32°34′42″	19	83	325
AS_92	$23^h57^m40.8^s$	–32°35′33″	15	48	189
AS_93	$23^h57^m43.9^s$	–32°34′32″	9	47	183
AS_94	$23^h57^m43.4^s$	–32°35′49″	8	33	130
AS_95	$23^h57^m37.3^s$	–32°35′37″	29	90	351
AS_96	$23^h57^m47.3^s$	–32°36′42″	18	70	274
AS_97	$23^h57^m37.6^s$	–32°36′4″	9	36	139
AS_98	$23^h57^m31.7^s$	–32°35′1″	7	23	89
AS_99	$23^h57^m44.1^s$	–32°32′36″	9	41	159
AS_100	$23^h57^m42.0^s$	–32°36′35″	23	104	405
AS_101	$23^h57^m44.8^s$	–32°34′42″	19	76	296
AS_102	$23^h57^m41.7^s$	–32°35′2″	26	93	362

Table 1. continued.

Name	α_{2000}	δ_{2000}	N	Size [μrad]	Size [pc]
AS_103	$23^h57^m42.2^s$	–32°33′52″	9	52	202
AS_104	$23^h57^m44.2^s$	–32°35′14″	12	59	232
AS_105	$23^h57^m43.0^s$	–32°36′18″	33	130	507
AS_106	$23^h57^m42.7^s$	–32°34′40″	21	80	314
AS_107	$23^h57^m41.5^s$	–32°35′24″	11	52	202
AS_108	$23^h57^m39.8^s$	–32°35′29″	7	41	160
AS_109	$23^h57^m42.9^s$	–32°33′30″	7	47	184
AS_110	$23^h57^m39.5^s$	–32°34′40″	16	61	238
AS_111	$23^h57^m40.3^s$	–32°34′50″	7	36	141
AS_112	$23^h57^m43.8^s$	–32°35′2″	20	94	369
AS_113	$23^h57^m41.1^s$	–32°36′29″	6	31	120
AS_114	$23^h57^m37.1^s$	–32°34′55″	16	69	270
AS_115	$23^h57^m35.0^s$	–32°35′32″	6	33	128
AS_116	$23^h57^m47.5^s$	–32°34′25″	8	45	176
AS_117	$23^h57^m46.1^s$	–32°36′32″	7	38	147
AS_118	$23^h57^m36.3^s$	–32°36′8″	14	65	253
AS_119	$23^h57^m45.0^s$	–32°34′4″	7	32	126
AS_120	$23^h57^m30.3^s$	–32°34′45″	23	73	285
AS_121	$23^h57^m41.3^s$	–32°36′56″	8	43	169
AS_122	$23^h57^m40.0^s$	–32°35′45″	7	31	122
AS_123	$23^h57^m40.5^s$	–32°36′22″	6	37	143
AS_124	$23^h57^m44.8^s$	–32°35′54″	6	28	109
AS_125	$23^h57^m47.2^s$	–32°35′53″	17	64	251
AS_126	$23^h57^m45.9^s$	–32°33′38″	12	61	238
AS_127	$23^h57^m45.2^s$	–32°35′22″	8	26	103
AS_128	$23^h57^m35.6^s$	–32°34′41″	6	24	93
AS_129	$23^h57^m42.7^s$	–32°35′31″	13	58	225
AS_130	$23^h57^m38.4^s$	–32°35′21″	9	42	163
AS_131	$23^h57^m45.3^s$	–32°34′14″	11	56	218
AS_132	$23^h57^m44.1^s$	–32°34′22″	9	43	167
AS_133	$23^h57^m42.7^s$	–32°35′10″	14	55	214
AS_134	$23^h57^m46.9^s$	–32°33′52″	16	73	284
AS_135	$23^h57^m45.3^s$	–32°36′31″	6	33	131
AS_136	$23^h57^m45.4^s$	–32°36′9″	6	32	123
AS_137	$23^h57^m42.6^s$	–32°32′33″	7	27	105
AS_138	$23^h57^m44.0^s$	–32°34′0″	6	32	123
AS_139	$23^h57^m44.9^s$	–32°35′2″	7	28	110
AS_140	$23^h57^m47.4^s$	–32°36′18″	6	24	93
AS_141	$23^h57^m43.0^s$	–32°33′40″	8	32	125
AS_142	$23^h57^m36.5^s$	–32°34′42″	7	36	142
AS_143	$23^h57^m36.1^s$	–32°34′15″	6	33	131
AS_144	$23^h57^m48.3^s$	–32°37′10″	6	46	179
AS_145	$23^h57^m44.9^s$	–32°37′35″	8	30	118
AS_146	$23^h57^m37.7^s$	–32°34′38″	6	26	103
AS_147	$23^h57^m41.8^s$	–32°34′17″	6	50	195
AS_148	$23^h57^m38.6^s$	–32°35′44″	6	27	106